

Dynamic oxygenation measurements using a phosphorescent coating within a mammary window chamber mouse model

Rachel Schafer^{1,3} and Arthur F. Gmitro^{1,2,3,*}

¹ Department of Biomedical Engineering, University of Arizona, 1657 E. Helen St., Tucson, AZ 85721, USA

² College of Optical Sciences, University of Arizona, 1630 E. University Blvd, Tucson, AZ 85721, USA

³ Department of Medical Imaging, University of Arizona, 1609 N Warren Ave, Tucson, AZ 85724, USA

*gmitro@radiology.arizona.edu

Abstract: Phosphorescent lifetime imaging was employed to measure the spatial and temporal distribution of oxygen partial pressure in tissue under the coverslip of a mammary window chamber breast cancer mouse model. A thin platinum-porphyrin coating, whose phosphorescent lifetime varies monotonically with oxygen partial pressure, was applied to the coverslip surface. Dynamic temporal responses to induced modulations in oxygenation levels were measured using this approach.

© 2015 Optical Society of America

OCIS codes: (170.3650) Lifetime-based sensing; (170.1470) Blood or tissue constituent monitoring.

References and links

1. P. Vaupel and A. Mayer, "Hypoxia in cancer: significance and impact on clinical outcome," *Cancer Metastasis Rev.* **26**(2), 225–239 (2007).
2. J. L. Tatum, G. J. Kelloff, R. J. Gillies, J. M. Arbeit, J. M. Brown, K. S. Chao, J. D. Chapman, W. C. Eckelman, A. W. Fyles, A. J. Giaccia, R. P. Hill, C. J. Koch, M. C. Krishna, K. A. Krohn, J. S. Lewis, R. P. Mason, G. Melillo, A. R. Padhani, G. Powis, J. G. Rajendran, R. Reba, S. P. Robinson, G. L. Semenza, H. M. Swartz, P. Vaupel, D. Yang, B. Croft, J. Hoffman, G. Liu, H. Stone, and D. Sullivan, "Hypoxia: importance in tumor biology, noninvasive measurement by imaging, and value of its measurement in the management of cancer therapy," *Int. J. Radiat. Biol.* **82**(10), 699–757 (2006).
3. P. L. Olive, J. P. Ban  th, and C. Aquino-Parsons, "Measuring hypoxia in solid tumours--is there a gold standard?" *Acta Oncol.* **40**(8), 917–923 (2001).
4. J. A. Raleigh, S.-C. Chou, G. E. Arteel, and M. R. Horsman, "Comparisons among Pimonidazole Binding, Oxygen Electrode Measurements, and Radiation Response in C3H Mouse Tumors," *Radiat. Res.* **151**(5), 580–589 (1999).
5. S. K. Chitneni, G. M. Palmer, M. R. Zalutsky, and M. W. Dewhirst, "Molecular imaging of hypoxia," *J. Nucl. Med.* **52**(2), 165–168 (2011).
6. X. Sun, G. Niu, N. Chan, B. Shen, and X. Chen, "Tumor hypoxia imaging," *Mol. Imaging Biol.* **13**(3), 399–410 (2011).
7. A. Nunn, K. Linder, and H. W. Strauss, "Nitroimidazoles and imaging hypoxia," *Eur. J. Nucl. Med.* **22**(3), 265–280 (1995).
8. P. Babilas, G. Liebsch, V. Schacht, I. Klimant, O. S. Wolfbeis, R.-M. Szeimies, and C. Abels, "In vivo phosphorescence imaging of pO₂ using planar oxygen sensors," *Microcirculation* **12**(6), 477–487 (2005).
9. R. I. Dmitriev and D. B. Papkovsky, "Optical probes and techniques for O₂ measurement in live cells and tissue," *Cell. Mol. Life Sci.* **69**(12), 2025–2039 (2012).
10. R. Schafer, H. M. Leung, and A. F. Gmitro, "Multi-modality imaging of a murine mammary window chamber for breast cancer research," *Biotechniques* **57**(1), 45–50 (2014).
11. S. P. Robinson, F. A. Howe, M. Stubbs, and J. R. Griffiths, "Effects of nicotinamide and carbogen on tumour oxygenation, blood flow, energetics and blood glucose levels," *Br. J. Cancer* **82**(12), 2007–2014 (2000).
12. J. L. H. Johnson, R. A. Leos, A. F. Baker, and E. C. Unger, "Radiosensitization of Hs-766T pancreatic tumor xenografts in mice dosed with dodecafluoropentane nano-emulsion – preliminary findings," *J. Biomed. Nanotechnol.* **10**, 1–8 (2014).
13. D. G. Hirst, G. D. Kennovin, and F. W. Flitney, "The radiosensitizer nicotinamide inhibits arterial vasoconstriction," *Br. J. Radiol.* **67**(800), 795–799 (1994).
14. J. H. A. M. Kaanders, J. Bussink, and A. J. van der Kogel, "ARCON: a novel biology-based approach in radiotherapy," *Lancet Oncol.* **3**(12), 728–737 (2002).

15. G. Helmlinger, F. Yuan, M. Dellian, and R. K. Jain, "Interstitial pH and pO₂ gradients in solid tumors in vivo: high-resolution measurements reveal a lack of correlation," *Nat. Med.* **3**(2), 177–182 (1997).
16. J. V. Moore, P. S. Hasleton, and C. H. Buckley, "Tumour cords in 52 human bronchial and cervical squamous cell carcinomas: Inferences for their cellular kinetics and radiobiology," *Br. J. Cancer* **51**, 407–413 (1985).
17. J. Pacheco-Torres, P. López-Larrubia, P. Ballesteros, and S. Cerdán, "Imaging tumor hypoxia by magnetic resonance methods," *NMR Biomed.* **24**(1), 1–16 (2011).
18. B. F. Jordan, J. Magat, F. Colliex, E. Ozel, A.-C. Fruytier, V. Marchand, L. Mignon, C. Bouzin, P. D. Cani, C. Vandeputte, O. Feron, N. Delzenne, U. Himmelreich, V. Denolin, T. Duprez, and B. Gallez, "Mapping of oxygen by imaging lipids relaxation enhancement: A potential sensitive endogenous MRI contrast to map variations in tissue oxygenation," *Magn. Reson. Med.* **70**(3), 732–744 (2013).
19. Z. Zhang, R. R. Hallac, P. Peschke, and R. P. Mason, "A noninvasive tumor oxygenation imaging strategy using magnetic resonance imaging of endogenous blood and tissue water," *Magn. Reson. Med.* **71**(2), 561–569 (2014).
20. M. Lovett, K. Lee, A. Edwards, and D. L. Kaplan, "Vascularization strategies for tissue engineering," *Tissue Eng. Part B Rev.* **15**(3), 353–370 (2009).
21. H. W. Hopf, T. K. Hunt, J. M. West, P. Blomquist, W. H. Goodson 3rd, J. A. Jensen, K. Jonsson, P. B. Paty, J. M. Rabkin, R. A. Upton, K. von Smitten, and J. D. Whitney, "Wound tissue oxygen tension predicts the risk of wound infection in surgical patients," *Arch. Surg.* **132**(9), 997–1004 (1997).

1. Introduction

Tumor hypoxia has important implications in terms of disease progression, aggressiveness, and treatment response [1,2]. The ability to measure hypoxia dynamically over time and spatially over the extent of a tumor would be a significant advance over the commonly utilized and accepted oxygen tension measurement techniques. Two of the most common approaches to oxygen measurement include insertion of pO₂ needle electrode probes and administration of nitroimidazoles (e.g., pimonidazole) [3,4]. The use of pO₂ probes is invasive, unreliable, and prone to variability and measurement bias based on probe location [5]. Nitroimidazoles are administered IV or IP and are subject to delivery limitations in reaching the target tissue site. In addition, nitroimidazoles only report on cells that have an intracellular pO₂ level below approximately 10 mmHg [4,6]. Visualization of nitroimidazoles requires removal of the tissue followed by immunohistochemical processing, sectioning and staining. Tissue biopsy is destructive and limited to a measurement at a single time point [5]. More recently, radiolabeled versions of nitroimidazoles have been developed [6,7]. While potentially this eliminates the need for tissue removal, the radiolabeled agent approach still presents a temporal snapshot of oxygenation levels and is dependent upon successful delivery of agent to the tissue of interest.

The development of alternative methods for detecting and measuring hypoxia is an active area of research. One approach has been the utilization of porphyrin molecules that change the rate of phosphorescence emission (lifetime), dependent on the amount of oxygen present. Oxygen acts as a quencher that decreases the phosphorescence lifetime [8]. Most *in vivo* studies have utilized intravascular probes, although there has been some development of probes measuring extracellular oxygenation outside of the vascular system [9]. The injected probes are cleared over time, limiting the time frame for monitoring. The probes generally have half-lives on the order of a few hours [9]. Babilas et al. have shown the ability to encapsulate platinum porphyrin molecules in a polymer matrix and coat it on the surface of a coverslip. The group demonstrated the approach using a titanium dorsal skin-fold window chamber hamster model for single baseline measurements [8]. This approach has potential to be utilized for repeatable measurements over the course of a week without the need for additional introduction of new probe. The encapsulation of the phosphorescent probe molecule in a polystyrene coating increases the time period over which adequate probe concentrations are present compared to injectable probes.

The work herein describes the first implementation and testing of a platinum-porphyrin coating applied to a mammary window chamber (MWC) model of breast cancer for dynamic oxygenation assessment. The MWC model that we have developed is orthotopic, allowing breast cancer tumors to develop in their natural environment, and does not impose restrictions on the development of the tumor in three-dimensions [10]. The MWC model allows for

localized regions of hypoxia to develop, making it a more realistic model of human breast cancer. The phosphorescent lifetime approach was used to dynamically detect physiologically induced oxygenation modulations over the spatial extent of the mammary tissue and tumor in contact with the coated coverslip. The concordance between the pO_2 estimates based on phosphorescence measurements and the visualization of hypoxia by standard pimonidazole immunohistochemical staining of tissue was evaluated. Additionally, measurements from both the phosphorescent lifetime coating and a fiber optic pO_2 probe were obtained from the same tumor.

2. Materials and methods

2.1 Mammary window chamber mouse model

We have developed and reported on a mammary window chamber (MWC) breast cancer mouse model that employs a custom plastic window chamber support structure and a removable coverslip [10]. For imaging pO_2 , platinum-porphyrin coated coverslips were placed either at the time of MWC implantation in the mouse or after removal of a standard 8 mm uncoated glass coverslip. Imaging was delayed for at least 24 hours after replacement with a coated coverslip to allow the tissue/coverslip interface to stabilize. The MWC structures were surgically implanted over seven day old tumors grown in the fourth mammary fat pad of eight female, post-breeder SCID mice. The tumors were created by injection of $1-5 \times 10^6$ MDA-MB-231/eGFP human breast cancer cells. Details of the surgical procedure and post-operative care were described previously [10]. All animal experiments and procedures were reviewed and approved by the University of Arizona Institutional Animal Care and Use Committee.

During all imaging experiments, the animals were anesthetized with 2% isoflurane before being placed in a supine position within an animal holder. Animals were then maintained on 1.0-1.5% isoflurane with a constant 1 L/min flow rate of medical-grade oxygen (or air) during imaging experiments. A custom holder supported the mice, while maintaining delivery of anesthesia, and minimizing movement of the window chamber structure. The animal temperature was monitored with a rectal temperature probe and maintained at $37^\circ\text{C} \pm 1^\circ\text{C}$ through the use of a heating pad placed beneath the animal holder.

2.2 Oxygen sensitive platinum-porphyrin coating

A 5 wt% solution of platinum-octaethyl-porphyrin (Pt-OEP) (Frontier Scientific, Logan, UT) to polystyrene (MW = 50 kDa) (Sigma-Aldrich, St. Louis, MO) was dissolved in chloroform, and then dispensed onto either large, 63.5 mm diameter round glass coverslips or small, 8 mm diameter round glass coverslips (No.1 thickness) for spin coating. The coverslips were cleaned with acetone and methanol prior to spin-coating. The solution was applied while the coverslip was stationary in the case of the small coverslips or spinning at a low speed (500 rpm) for the larger coverslips. Enough solution was added to cover over half of the area of the coverslip. The speed of the Solitec spin coater was increased to 2000 rpm for 25 seconds to spread the solution in a uniform thickness layer over the entire coverslip area. When using the larger coverslips, approximately 8 mm diameter coverslips were cut from the larger coverslip using a diamond-coated hole-cutter bit. The coating thickness was measured to be $1.7\ \mu\text{m}$, as measured using a profilometer. The coated coverslip was placed in the MWC structure with the coated side in direct contact with the tissue.

2.3 Phosphorescent lifetime instrumentation and imaging procedure

A tunable optical parametric oscillator (OPO) pumped by a Nd:YAG Q-switched laser with 20 Hz pulse repetition rate and 3 ns pulse width was used to produce optical pulses at a wavelength of 532 nm. An Olympus MVX10 scientific microscope with a 595 nm dichroic and 645/75 nm emission filter was used for imaging the fluorescence emission from the

coated window chamber structure. An interline CCD camera (Photonics Research Systems) with 596 x 796 pixels and on-chip integration, was used to capture time-gated images for estimating the lifetime of the Pt-OEP phosphorescence emission across the image field.

A series of 14 images was acquired with 5 μ s gate width at increasing delay times, ranging from 0 to 65 μ s in 5 μ s increments after the end of the laser pulse. The laser sends a signal to the pulse generator to synchronize the timing. The pulse generator waits the designated delay time before sending a signal to the camera controller to begin the exposure. Prior to processing, images were down-sampled using 2x2 pixel binning to increase SNR and decrease data processing time. The phosphorescent lifetime for each voxel was obtained by fitting the temporal evolution of the signal intensities to a single mono-exponential decay. Lifetime maps were generated as images of the pixel lifetime estimates.

Conversion between phosphorescent lifetime values and pO_2 was based on a two point calibration procedure, since previous characterization of these coatings reported a linear response [8]. A linear calibration fit was made for the lifetimes of two measurements, one with exposure of the coverslip to air ($pO_2 = 140$ mmHg) and the other with exposure of the coverslip to a zero dissolved oxygen solution (Rica Chemical Company, Arlington, TX), containing sodium sulfite ($pO_2 = 0$ mmHg). Average lifetime values of 57.4 μ s (± 2.45 μ s) were measured under exposure to the zero dissolved oxygen solution: lifetime values of 16.5 μ s (± 1.11 μ s) were measured under air exposure.

Wide-field fluorescence images of the GFP transfected tumors within the MWC were captured on the same Olympus MVX10 scientific microscope. The GFP tumor signal was acquired by setting the OPO laser emission to 488 nm and using an appropriate GFP filter set on the microscope.

2.4 Oxygen modulation with gas modification

Two animals were stabilized for baseline measurements of the tissue oxygenation state by breathing air with isoflurane gas for 15 minutes. After acquiring the baseline measurements, the gas flow was replaced with oxygen. The flow of oxygen with isoflurane was maintained for approximately 15 minutes before switching back to air. Multiple lifetime measurements were acquired during the switch to oxygen as well as during the recovery period when the anesthesia gas returned back to air. The opposite experiment (oxygen to air and back to oxygen) was also performed.

2.5 Oxygen modulation with pharmaceutical agents

The pO_2 in tissue was also modulated using pharmaceutical agents. Three animals were stabilized for baseline measurements under air or oxygen gas plus isoflurane anesthesia. In one set of experiments, an intraperitoneal injection of 1000 mg/kg body weight nicotinamide (Sigma Aldrich, St. Louis, MO) was administered. Nicotinamide inhibits blood vessel constriction and thus allows more oxygen to be delivered to oxygenate tissue [11]. In another set of experiments, an intravenous injection of 0.6 mL/kg body weight NVX-108 (NuvOx Pharma, Tucson, AZ) was administered. NVX-108 is an investigational therapeutic composed of a nano-emulsion of 2% w/vol dodecofluoropentane that binds significant oxygen and increases delivery of oxygen to tissue [12].

2.6 Pimonidazole staining

Hypoxia staining was performed in two animals by administering hypoxyprobe (pimonidazole hydrochloride) i.p. at 60 mg/kg animal body weight. The animals were euthanized one hour after hypoxyprobe was administered. The tissue beneath the MWC was harvested and placed in 10% formalin in phosphate buffered saline to prepare it for immunohistochemistry processing. Within 24 hours, the tissue was transferred to 70% ethanol before being embedded in paraffin. Tissue slices were stained with anti-pimonidazole mouse monoclonal antibody.

2.7 Oxygen probe measurement

An OxyLab fiber optic based oxygen probe (Oxford Optronics, Abingdon, United Kingdom) was inserted into the mammary fat pad in two anesthetized mice after the termination of phosphorescent lifetime imaging experiments. The location of the probe was varied and measurements were recorded over the course of several minutes in each location. The probe location relative to the tumor location was also recorded. The temperature of the animal was monitored and the OxyLab system was updated with the body temperature to compensate for temperature variation in the calibration of the probe.

3. Results

The 2D pO_2 maps derived from the measured lifetime maps show the underlying spatial variation of the tissue oxygenation. A GFP image and a corresponding pO_2 image of a MWC with a large tumor are shown in Fig. 1. The tumor (bright GFP signal in Fig. 1(a)) boundary is shown by the dark outline in the GFP and pO_2 images. In this image the pO_2 is lower in the majority of the GFP tumor compared to the normal tissue surrounding the tumor.

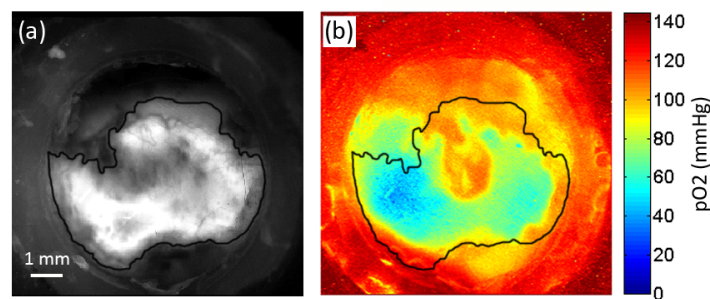


Fig. 1. GFP tumor with corresponding pO_2 map. Tumor location based on GFP signal (a) correlates with the spatial variation of the pO_2 map (b), indicating low pO_2 values within the tumor.

As described in the methods, multiple experiments were performed where tissue oxygenation levels were modulated. This was done to demonstrate the ability of the MWC coating to measure physiologically relevant changes in tissue pO_2 *in vivo*.

3.1 Modulation with gas

Phosphorescence lifetime maps and subsequent pO_2 maps were derived from data acquired while the gas mixture of isoflurane anesthesia was modified. The experiment was repeated in three animals. A representative result is shown in Fig. 2. In this particular window chamber, no significant difference in tissue oxygenation was observed between the tumor (outlined in black) and surrounding regions of normal tissue, although there was significant spatial heterogeneity in the distribution of tissue pO_2 . The baseline lifetime map while the animal was breathing air (Fig. 2(a)) with a flow rate of 1 L/min was repeated three times and produced a consistent pO_2 distribution pattern. Lifetime values in specific regions of interest fluctuated within a range of 6 μ s in the three repeated measurements. The anesthesia gas was then switched to oxygen at the same 1L/min flow rate. Lifetime and pO_2 maps were derived from the data collected over the 15 minutes during which oxygen was administered. The results showed a significant drop in lifetime values corresponding to increased tissue oxygenation. The percent pO_2 rose between 22 and 43% compared to baseline measurements while breathing air. After returning the animal to breathing air, the pO_2 maps showed a progressive decrease in pO_2 . The pO_2 did not return back fully to the baseline values over the 15 minutes of repeat measurement in all regions. The mean lifetime and pO_2 values in three regions of interest at the acquired time points are displayed in the graph in Fig. 2(d). The

entire tumor region, as identified by GFP fluorescence signal (outlined in black), did not respond in a significantly different manner compared to other tissue locations. It can be seen from the pO_2 values that this tumor is not hypoxic.

Experiments performed in the opposite order of oxygen to air to oxygen (data not shown), demonstrate the opposite change in pO_2 as expected. Based on experiments modulating the gases in both directions (air to oxygen to air and oxygen to air to oxygen), the introduction of oxygen produces a shortening of the lifetime measurement consistent with higher tissue pO_2 . It was observed that the tissue responds slightly more rapidly to an increase in oxygen in the anesthesia gas than the reverse decrease in oxygen in the anesthesia gas.

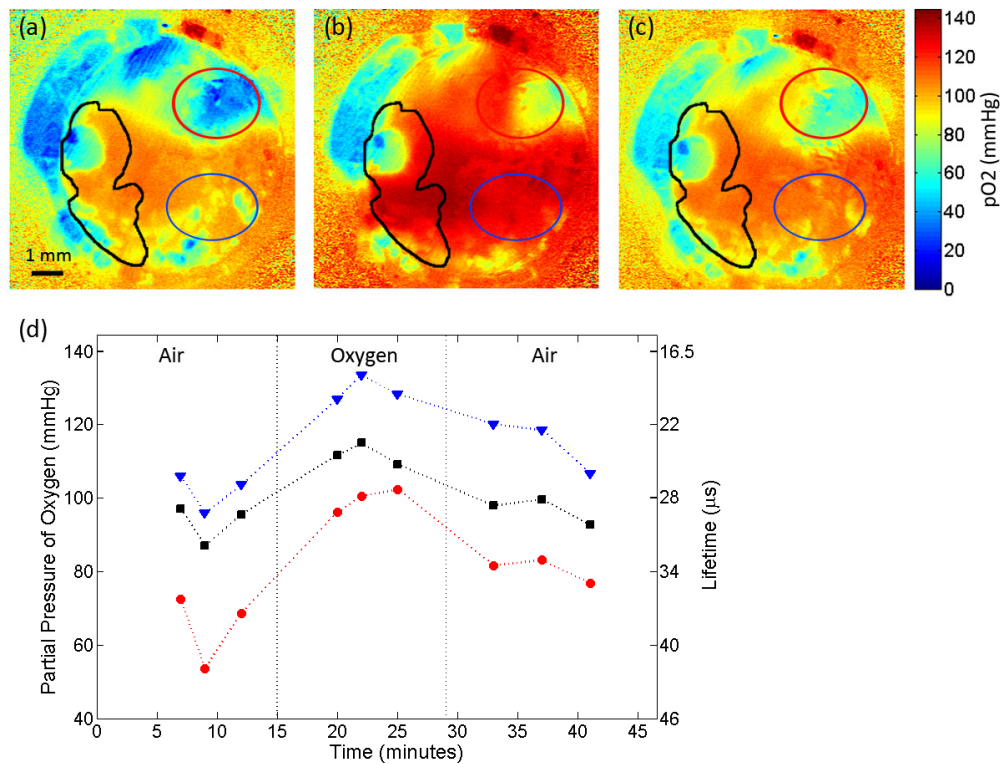


Fig. 2. Modulation of tissue pO_2 with anesthesia delivery gas. pO_2 maps acquired while the mouse breathed (a) air with isoflurane, (b) oxygen with isoflurane for 15 minutes, and (c) back to air with isoflurane for 10 minutes. (d) The average lifetime and pO_2 values within the tumor (black) and two normal tissue regions (designated in the pO_2 maps by red and blue outlines) acquired over the course of the modulation experiment.

3.2 Modulation with nicotinamide

In another modulation experiment, lifetime data were acquired before and after the administration of nicotinamide. Nicotinamide acts to prevent vasoconstriction and thus maintains or in some cases increases oxygen delivery depending on the state of vasoconstriction in the blood vessels [13]. Nicotinamide has been explored through clinical trials as a means to address chronic and acute hypoxia prior to radiotherapy [14]. The baseline pO_2 map obtained while the animal was breathing oxygen with isoflurane anesthesia is shown in Fig. 3(b). The tumor location was determined by the GFP image shown in Fig. 3(a). The outline of the tumor (black) is superimposed on the pO_2 maps. The pO_2 maps from data acquired 3, 8, 19, and 78 minutes after administration of nicotinamide are shown in Fig. 3(c)-3(f). The temporal response both within the tumor (black and blue outlined regions of interest)

and in normal tissue (red outlined region of interest) are shown in Fig. 3(g). The i.p. injection of nicotinamide resulted in a significant rise in the pO_2 values in normal regions of the tissue. The tumor region also increased in pO_2 values, but the average increase was less than in the surrounding normal tissue. There is a lack of smooth muscle in tumor vasculature, and this lack of vascular smooth muscle would result in a lower response to a drug inhibiting vasoconstriction. This may explain the decreased effect of nicotinamide within the tumor region.

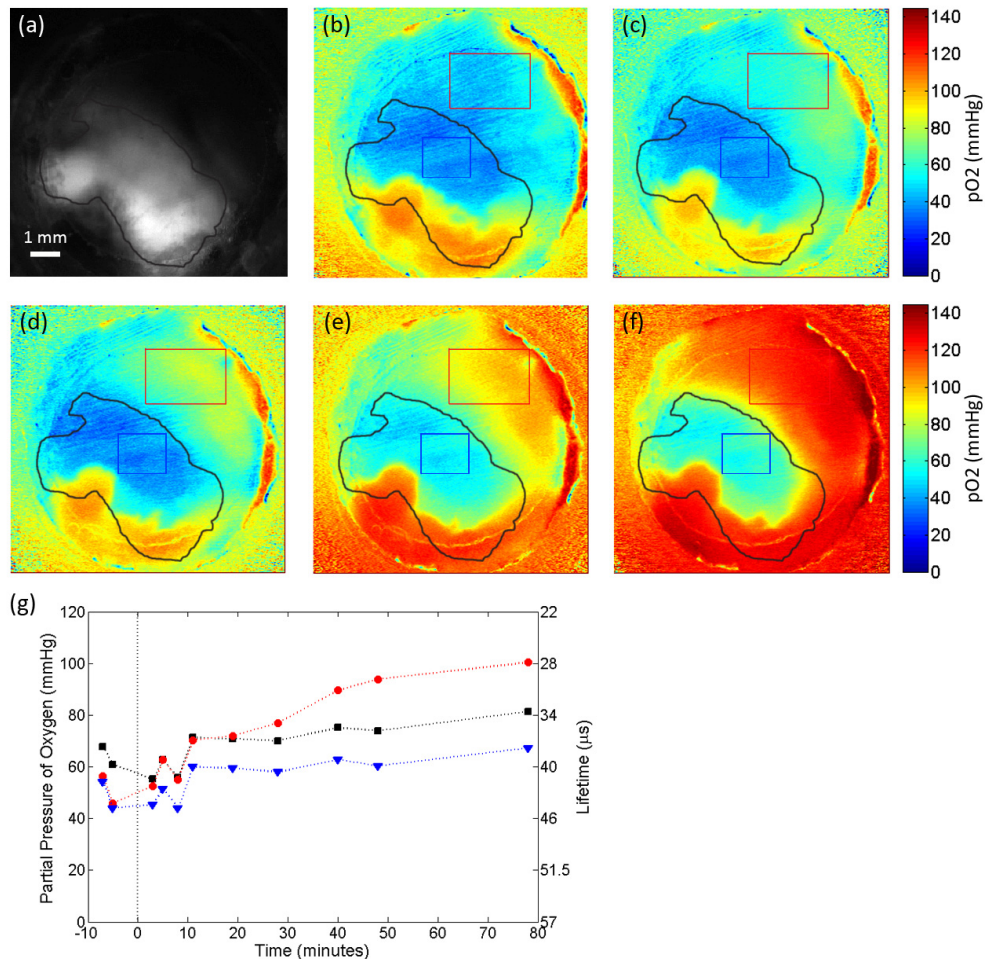


Fig. 3. Modulation with nicotinamide. (a) The GFP tumor signal within the MWC is outlined on the pO_2 maps. (b) pO_2 maps were acquired in a MWC animal under stable conditions while it was breathing oxygen with isoflurane anesthesia. An i.p. injection of nicotinamide was administered to increase oxygenation, pO_2 maps acquired at (c) 3, (d) 8, (e) 19 and (f) 78 minutes after injection show a steady increase in pO_2 within the tissue. (g) The dynamic temporal changes in average lifetime and pO_2 values within the tumor (black and blue regions of interest) and in the normal tissue (red region of interest) following nicotinamide administration at time $t = 0$.

3.3 Modulation with NVX-108

Another way to alter tissue oxygenation is through delivery of oxygen carrying drugs. NVX-108 is one such drug under development for increasing oxygenation of hypoxic tumors prior to radiation treatment. The drug has completed preliminary testing in a pancreatic xenograft model, and has moved onto a clinical trials in the context of treating gliomas [12]. The drug

has potential for expanding into other common hypoxic tumor types, including breast cancers. NVX-108 was administered IV to a MWC animal on two occasions, one while the animal breathed oxygen with isoflurane anesthesia and the other while the animal breathed air with isoflurane anesthesia. The results of the experiment with oxygen are shown in Fig. 4. Three baseline measurements were acquired prior to the IV injection of NVX-108 one of which is shown in Fig. 4(b). The tumor location was determined based on the GFP image (Fig. 4(a)) and the outline of the tumor (black) is superimposed on the pO_2 maps. Several lifetime measurements were acquired over an hour following the injection. Select pO_2 maps from data acquired 3, 10, 18 and 40 minutes after administration of agent are displayed in Fig. 4(c)-4(f). The pO_2 rose significantly in the first few minutes following administration of the drug and remained elevated for the entire 63 minute monitoring period. The decrease in the lifetime values (increase in pO_2) is consistent with enhanced delivery of oxygen to the tissue and is in agreement with unpublished findings obtained by NuvOx Pharma showing an increase in pO_2 as measured with an oxygen electrode probe. The results with the animal breathing air were similar, but the magnitude of the response was less than with oxygen. This finding is interesting in that a high oxygen concentration in the blood appears to increase the effectiveness of this drug, presumably by allowing the agent to remain more fully saturated with oxygen during delivery to tissue.

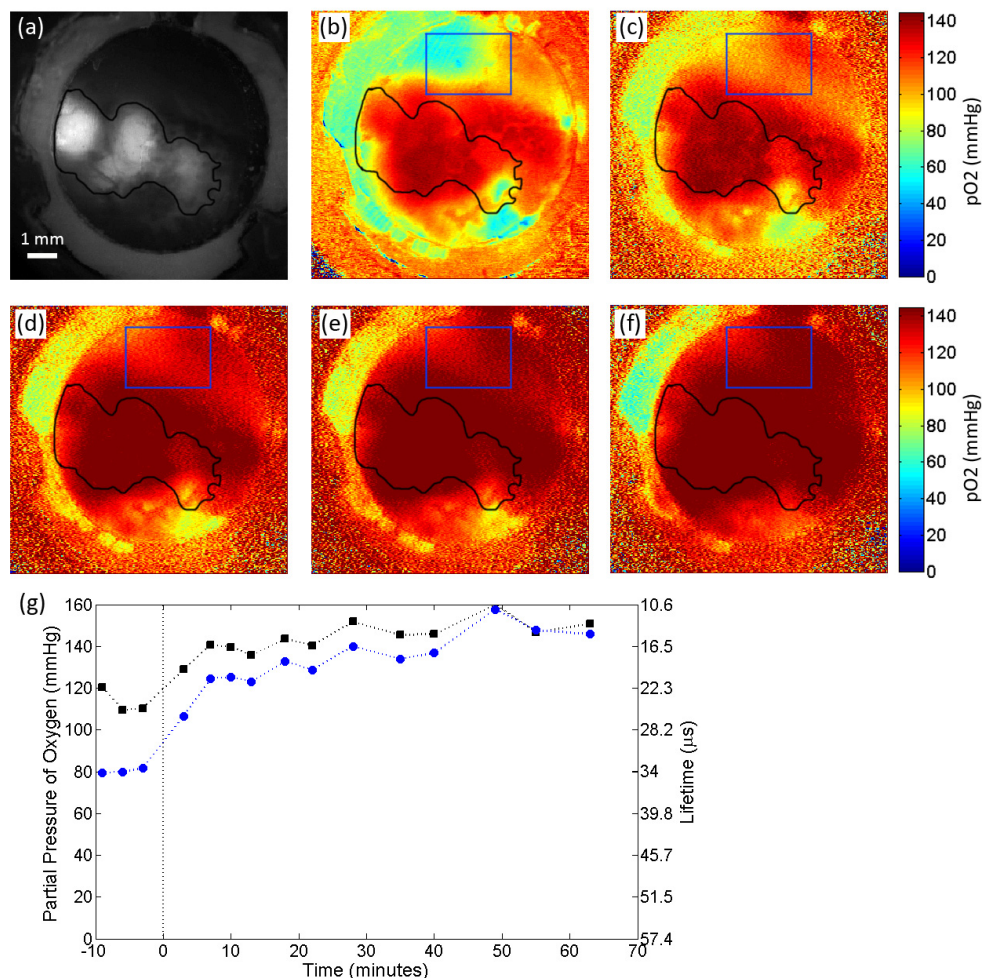


Fig. 4. Oxygen delivery to tissue with the investigational pharmaceutical, NVX-108. (a) GFP tumor signal in the MWC. (b) Baseline pO₂ map acquired while the animal breathed oxygen with isoflurane anesthesia. Following administration of 0.6 mL/kg body weight NVX-108 into the tail vein, subsequent pO₂ maps acquired at (c) 3, (d) 10, (e) 18 and (f) 40 minutes show a rapid and sustained rise in pO₂ values. (g) The dynamic temporal changes in average lifetime and pO₂ values within the tumor (black outlined region of interest) and in the normal tissue (blue outlined region of interest) following NVX-108 administration at time t = 0.

3.4 Pimonidazole staining of tissue

Figure 5(a) shows a pO₂ map of one animal where the pO₂ within the tumor (black outline) is uniformly low and in a range that would indicate it is close to being hypoxic. In this animal, pimonidazole was administered after the phosphorescence lifetime imaging measurement. The tissue from the mammary fat pad region was harvested after the animal was euthanized. The paraffin-embedded tissue was processed and cut in slices oriented perpendicular to the tissue surface in contact with the coverslip of the window chamber. An image of the processed slide is shown in Fig. 5(b). The brown staining, positive for pimonidazole and indicative of cells with a pO₂ less than 10 mmHg, is clearly seen within the tumor. However, the staining is heterogeneous in its distribution with some areas of the tumor showing a higher degree of staining than others both at the surface (upper boundary of Fig. 5(b)) and deeper inside the tumor. Variability in pimonidazole staining can be due to how well perfused the

tissue is, as well as the degree of hypoxia, since the stain has to reach the tissue of interest to show that it is hypoxic. An advantage of the lifetime approach to measuring hypoxia is that it does not depend on the tissue concentration of a delivered agent. A histogram of the pO_2 values within the outlined tumor region is displayed in Fig. 5(c). The peak in the distribution of values measured by the coating falls within 10-15 mmHg. These values are right at the edge of the reported positive detection threshold for pimonidazole. The average pO_2 over the entire tumor region of interest in Fig. 5(a) is 26.8 mmHg. The pimonidazole image shows that the tissue is mildly stained near the surface with the highest degree of staining in the middle (arrow) consistent with the lower pO_2 in the center of the tumor on Fig. 5(a). The correlation with an accepted method of assessing hypoxia provides evidence that the lifetime measurement approach is yielding a quantitative spatially and temporally resolved evaluation of tissue hypoxia without removal of the tissue at least at the contact surface of the coverslip.

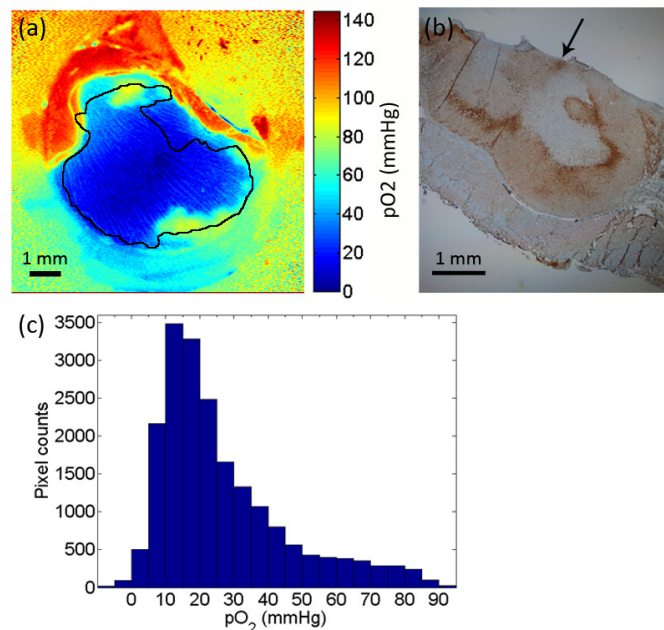


Fig. 5. Comparison of phosphorescent lifetime and pimonidazole hypoxia measurement assays. (a) The pO_2 measurement in the MWC indicates hypoxic conditions. (b) The corresponding pimonidazole staining of a slice of tissue perpendicular to the measured surface shows positive (brown) staining along a portion of the top surface that was in contact with the coating (arrow). (c) The histogram of pO_2 values within the black outlined tumor region in (a).

3.5 Coating stability

The stability of the coating is an important consideration for longitudinal studies monitoring oxygenation changes in tissue. In the imaging experiments, the coatings remained intact for at least a week after placement. After approximately a week, some local areas of the coatings did begin to break apart and become detached from the coverslip. Imperfections or scratches in the coating appear to lead to more rapid degradation. While coatings were observed to partially degrade in spots, the coating could be visualized and measurements obtained from the intact regions of the coating on the coverslip. Due to the unique design of the window chamber, the coverslip can be replaced with a new coverslip in the event the coating becomes significantly degraded. Following the termination of *in vivo* experimentation, a used coated coverslip was retested with the two-point lifetime calibration method. The coating was essentially unchanged under exposure to air, with a moderate change in the lifetime measurement acquired for the zero dissolved oxygen condition for the one coating tested. The

difference in the mean lifetime values during exposure to air for a fresh and used coating was $0.88\ \mu\text{s}$, equivalent to 3.01 mmHg change in pO_2 . The difference in the mean lifetime values during exposure to a zero dissolved oxygen solution for a fresh and used coating was $2.93\ \mu\text{s}$, equivalent to 10.03 mmHg change in pO_2 . The long term variability with the zero dissolved oxygen solution was approximately a factor of 2 larger than the short term variability observed with multiple repeat measurements at the initial time point.

3.6 Oxygen probe measurement

Limited testing was also performed with an OxyLab fiber optic based oxygen probe. In one animal, the probe was placed into the tissue, after removal of the window chamber structure. The probe results largely corroborated the high pO_2 values observed with the phosphorescent coating lifetime technique. Placement of the oxygen probe into the tumor at two spots gave average readings of $87.6 \pm 9.37\ \text{mmHg}$ and $90.95 \pm 3.94\ \text{mmHg}$. Measurements using the phosphorescent coating in this same general region of the tumor one day prior gave an average pO_2 value of $127.4 \pm 2.83\ \text{mmHg}$. A large amount of variability exists in the pO_2 measurements obtained with the fiber optic probe, depending on location and depth of the probe in the tissue. Additionally, the point readings with the fiber probe often were not very stable, exhibiting either a slow drift or larger transitions in the readings over a few minutes of monitoring. A temporally variable point measurement is not an ideal standard for comparison, but does tend to show consistency with the high oxygen partial pressure values measured with the phosphorescent coating. Both the phosphorescent lifetime and fiber optic probe measurement approaches yield pO_2 values higher than what has generally been reported in the literature for breast tissue and tumors. However, the measurement approaches are consistent and appear reliable based on calibration measurements.

4. Discussion

In this work we evaluated the use of a platinum porphyrin in polystyrene coating for its utility in measuring tissue oxygenation in an orthotopic breast cancer window-chamber mouse model. The ability to detect physiologically induced oxygenation changes was clearly demonstrated through multiple means of oxygenation modulation. Both static and modulated measurements of tissue oxygenation are feasible with a rapid response to tissue oxygenation changes under modulated conditions. The raw data for calculation of a lifetime map can be acquired in less than one minute with the current setup. This could be done even faster with fewer temporal measurements along the phosphorescence decay curve or with high laser power and shorter integration times. Data processing to create pO_2 maps from the signal decay measurements was done off-line, but this step could be incorporated into the processing pipeline to directly observe oxygenation changes in real time with a temporal resolution of a few seconds if necessary. The coatings were generally observed to be robust and stable for multiple days, making the approach suitable for longitudinal studies as well as for dynamic short term monitoring of tissue oxygenation or the detection of cycling hypoxia. To affirm the validity of the coating approach, oxygenation measurements were compared with a well-established pimonidazole staining protocol and with a fiber optic oxygen probe. The immunohistochemical staining observed in Fig. 4 confirms the tumor tissue in the MWC model can become hypoxic with reasonable concordance among measurements at the low end of pO_2 . At the higher pO_2 , the oxygen probe measurement was somewhat lower than that obtained in the coating. However, the accuracy of oxygen probe measurements is prone to error due to the invasive disruptive nature of the measurement. The coating approach supplies a well calibrated and non-invasive measurement of tissue oxygenation.

One limitation of the coated coverslip approach is that it is sensitive to only the top surface layer of tissue. The diffusion limit of oxygen in tissue is reported to be approximately 200 microns [15,16]. The phosphorescent coating is likely, therefore, only measuring average oxygen levels from the first 100-200 micron depth of the tissue below the coating. The

diffusion of oxygen may also explain why oxygenation maps have relatively smooth spatial variations across the extent of the MWC. However, while the majority of the collected phosphorescent signal is from direct emission from the coating which is imaged with high spatial resolution, some phosphorescence light propagates into the tissue and can backscatter before being detected. The light spread due to scattering of the phosphorescent signal could be another source of spatial blurring of the measured spatial distributions. In some instances, it is suspected that a thin fluid layer existed between the tissue and coating. However, because of oxygen diffusion, the experimental measurements almost certainly reflect to some degree the oxygen present in the tissue surface layer. The oxygenation modulation experiments showed changes concordant with systemic physiological alterations expected with, gas modulations, nicotinamide and the pharmaceutical agent, NVX-108.

It is worth noting, that the MWC model is compatible with multi-modality imaging and would therefore allow comparison and validation of techniques under development for tissue oxygenation assessment, including those employing new magnetic resonance imaging techniques [17–19]. The phosphorescent coating technique could have application in other non-window chamber applications where oxygenation measurements are beneficial. For example, the viability and success of tissue engineering constructs, as well as skin grafts, depends on sufficient oxygen delivery [20]. The coating approach might be applied to an area of a skin graft to provide insight into viability based on an oxygenation measurement. Oxygenation measurements could aid in wound healing assessments and the need for further debridement of dead or under perfused tissue from wound sites [21].

The current, commonly accepted methods for measuring pO_2 are by no means ideal for monitoring oxygenation. Oxygen probes are difficult to position precisely, can be unstable, and provide only a point measurement. Nitroimidazoles report a single time point and do not provide absolute pO_2 readings. The presented phosphorescent lifetime coating approach was investigated for its suitability in performing repeated, dynamic assessments of absolute pO_2 values in a straightforward noninvasive manner. Overall, the technique is a viable tool and can be usefully applied to the mammary window chamber for studying fluctuations in oxygenation.

Acknowledgments

This work was supported by the University of Arizona Cancer Center Fenton Maynard Endowment supporting Dr. Gmitro's research in cancer imaging. We would like to thank Dr. Marek Romanowski for allowing use of his laser and lifetime imaging equipment for these experiments. We would like to acknowledge the University of Arizona Cancer Center's Experimental Mouse Shared Resource for performing the animal surgeries, and the Tissue Acquisition and Molecular Analysis Shared Resource for preparing the immunohistochemistry slides. We would also like to thank the Center for Gamma Ray Imaging for operation and maintenance of the rapid prototyping printer used to make the window chamber structures and animal holders. We also acknowledge NuvOx Pharma for providing us with the investigational drug, NVX-108, and assistance in the experimental studies using the drug.